Numerical Simulation of Reinforced Soil Structures During Blast Loads

M. YOGENDRAKUMAR AND R. J. BATHURST

A comprehensive approach to the dynamic response analysis of reinforced soil structures subjected to blast loading is presented. The method is based on an estimate of the pressure-time response at the boundaries of target structures using a two-dimensional versatile gas dynamic code (SPLIT2D). The soil-reinforcement response is simulated using a direct nonlinear approach that is implemented in the finite element computer program RESBLAST. Examples of this approach to investigate the response of a reinforced soil wall and a soil slope with and without reinforcement are presented. The results of rapid cyclic tensile loading tests are used to obtain mechanical properties used in the nonlinear reinforcement model implemented in the finite element code.

Advanced polymeric material such as geogrids and geotextiles are becoming a common reinforcing material for the construction of reinforced soil systems used in industrial and military applications (*1*,*2*). Soil retaining walls and steepened slopes are often used in military and civilian applications to protect personnel, property, and adjacent structures from accidental detonation of stored explosives, munitions, and ammunition plants and to provide blast containment of volatile liquids. As in conventional reinforced soil structures, the advantages of polymeric-reinforced soil structures lie in their cost-effectiveness, rapid construction, minimization of ground area, and high tolerance of differential settlements. Less well understood is the dynamic response of these structures to short duration excitations resulting from above-ground explosions.

Related work on the seismic response of similar structures under earthquake excitation provides a starting point for the study of resistance to air blast. For earthquake design, the stability of steepened slopes and walls is usually estimated using analytical methods that are typically extended versions of conventional limit-equilibrium methods (*3*,*4*). These methods are primarily stress based and do not consider deformations explicitly.

More recently, the finite element method of analysis has been used to study the response of reinforced soil systems to dynamic loads (*5*–*9*). These papers have focused on the response due to earthquake excitations. The choice of excitation forces in earthquake simulations is relatively straightforward. The analogous task for air blast loading requires separate analyses that are complex and at least as computational intensive as the simulation of structure response alone.

To carry out numerical simulation of blast loadings on a reinforced soil system, it is necessary to establish the pressure-time history at the boundaries of the target structure. In this study the pressure-time history of air blast loadings was calculated using a computer package called SPLIT2D (*10*). The stress-deformation-time response of an example reinforced soil wall and steepened slope due to the boundary excitations predicted in the air blast simulation was carried out using the computer program RESBLAST (RESponse to BLAST loading) (*11*). RESBLAST implements a direct nonlinear method in which the nonlinear dynamic behavior of both the soil and the polymeric reinforcement are modeled. The behavior of soil in shear and the load-deformation behavior of the polymeric reinforcement are both assumed to be nonlinear, hysteretic, and to exhibit Masing behavior during unloading and reloading. A unique feature of this program is that permanent deformations are computed directly.

The retaining wall example was studied to examine the effect of magnitude of blast loading on structure response at different locations within the reinforced soil zone. The slope example was examined with and without reinforcement to investigate the influence of the polymeric reinforcement on the response of otherwise identical structures. The model parameters for the polymeric reinforcement were obtained from results of in-isolation, high-frequency, cyclic-loading tests.

METHOD OF ANALYSIS

In the current study, the procedure for computing the blast response of example target structures was carried out in two stages: first, the blast loading on the particular structure was determined using the computer program package SPLIT2D; next, the response of the structure to the boundary pressure-time loading was computed using the computer program RESBLAST.

Program SPLIT2D

SPLIT2D is a two-dimensional versatile gas dynamic code capable of solving a variety of problems involving blast, reactive flows, and interaction of shocks with obstructions. The governing equations are derived from the more general Navier-Stokes relations by eliminating the turbulence and diffusive transport terms. The resulting set of coupled partial differential relationships comprise continuity, momentum conservation, and energy conservation equations. The ideal gas equation of state relating the internal energy to the pressure and density is also used. The numerical algorithm uses an explicit time stepping algorithm. The spatial derivatives are discretized on a finite difference grid using a second-order

M. Yogendrakumar, Golder Associates Ltd., 224 West 8th Avenue, Vancouver, British Columbia, Canada V5Y 1N5. R. J. Bathurst, Department of Civil Engineering, Royal Military College of Canada, Kingston, Ontario, Canada K7K 5L0.

scheme in conjunction with the flux-corrected transport algorithm. Complicated geometries of the protective structures are set up by placing obstructions within the computational blast domain using rectangular, elliptical, and triangular shapes that can be superimposed. Similarly, regions with different initial conditions are created using these three shapes.

In this study the air blast was modeled as a planar wave front traveling horizontally until impact with the structure. The postimpact blast response in the surrounding space was determined by the magnitude and duration of the blast and the geometry of the obstruction.

Program RESBLAST

RESBLAST uses a direct nonlinear method that is implemented in a code for total stress analysis of reinforced soil structures subject to blast loading. The treatment of soil behavior under dynamic loading is based on algorithms originally implemented in program TARA-3 (*12*) developed by researchers at the University of British Columbia. In both programs an incremental approach has been adopted to model nonlinear behavior of soil using tangent shear and tangent bulk moduli, G_t and B_t, respectively. The incremental displacements during the blast loading are obtained by solving the incremental dynamic equilibrium equations given in Equation 1 by a direct numerical integration method.

$$[M]\{\Delta\ddot{x}\} + [C]\{\Delta\dot{x}\} + [K]\{\Delta x\} = \{\Delta P\} \tag{1}$$

Here $[M]$ is the mass matrix; $[C]$ is the damping matrix; $[K]$ is the stiffness matrix; $\{\Delta\ddot{x}\}$, $\{\Delta\dot{x}\}$, and $\{\Delta x\}$ are incremental acceleration, velocity, and displacement vectors of the nodes relative to the base; and $\{\Delta P\}$ is the increment in blast load.

The stiffness matrix $[K]$ is a function of the current tangent moduli during loading, unloading, and reloading. The use of shear and bulk moduli allows the elasticity matrix $[D]$ to be expressed as

$$[D] = B_t[Q_1] + G_t[Q_2] \tag{2}$$

where $[Q_1]$ and $[Q_2]$ are constant matrices for the plane strain conditions considered in the analysis. This formulation reduces the computation time for updating $[D]$ whenever G_t and B_t change in magnitude because of straining.

Soil Model

The behavior of soil in shear is assumed to be nonlinear and hysteretic and to exhibit Masing behavior during unloading and reloading. Masing behavior is a term used in mechanics to describe the pattern of hysteretic load/unload-strain cycles having the generic shape shown in Figure 1a. The relationship between shear stress τ and shear strain γ for the initial loading phase under loading conditions is assumed to be hyperbolic and given by

$$\tau = f(\gamma) = \frac{G_{max}\,\gamma}{[1 + (G_{max}/\tau_{max})|\gamma|]} \tag{3}$$

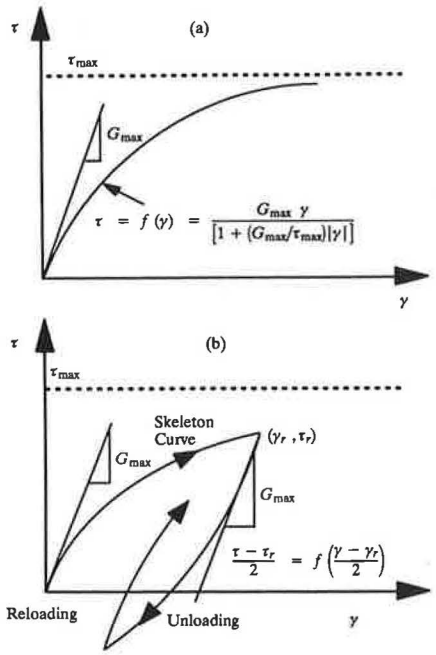

FIGURE 1 Nonlinear hysteretic loading paths for granular soil.

where G_{max} is the maximum shear modulus and τ_{max} is the maximum shear strength. The initial loading curve is shown in Figure 1a. The equation for the unloading curve from a point (γ_r, τ_r) at which the loading reverses direction is given by

$$\frac{\tau - \tau_r}{2} = f\left(\frac{\gamma - \gamma_r}{2}\right) \tag{4}$$

or

$$\frac{\tau - \tau_r}{2} = \frac{G_{max}\,(\gamma - \gamma_r)/2}{[1 + (G_{max}/2\tau_{max})|\gamma - \gamma_r|]} \tag{5}$$

The shape of the unloading-reloading curve is shown in Figure 1b. The tangent shear modulus, G_t, for a point on the skeleton curve is given by

$$G_t = \frac{G_{max}}{[1 + (G_{max}/\tau_{max})|\gamma|]^2} \tag{6}$$

and at a point on an unloading or reloading curve G_t is given by

$$G_t = \frac{G_{max}}{[1 + (G_{max}/2\tau_{max})|\gamma - \gamma_r|]^2} \tag{7}$$

The dynamic shear modulus, G_{max}, of the soil elements is calculated using the expression proposed by Seed and Idriss (*13*) as

$$G_{max} = 21.7\,K_{2max}\,P_a\left(\frac{\sigma_m}{P_a}\right)^{\frac{1}{2}} \tag{8}$$

where P_a is the atmospheric pressure in units consistent with mean normal stress σ_m and G_{max} and K_{2max} is a constant.

The response of the soil to uniform all-round pressure is assumed to be nonlinear elastic and dependent on the mean normal stress. Hysteretic behavior, if any, is neglected in this mode. The tangent bulk modulus, B_t, is expressed in the form

$$B_t = K_b P_a \left(\frac{\sigma_m}{P_a}\right)^n \tag{9}$$

where K_b is the bulk modulus constant and n is the bulk modulus exponent.

Reinforcement Model

The reinforcement is modeled using one-dimensional beam elements with axial stiffness only. Slip elements of the type developed by Goodman et al. (*14*) may be used to allow for the relative movements between the soil and reinforcement during dynamic loading. The behavior of relatively extensible reinforcement such as polymeric materials is assumed to be nonlinear. The relationship between axial load and axial strain for the initial loading is expressed in hyperbolic form as

$$F = \frac{D_i \varepsilon_a}{[1 + (D_i/F_m)|\varepsilon_a|]} \tag{10}$$

where

F = axial load per unit width (e.g., kN/m),
D_i = initial load modulus,
ε_a = axial strain, and
F_m = maximum axial strength.

The same model can be used to represent relatively inextensible types of reinforcement such as steel strips (elastic-perfectly plastic materials) by selecting fictitiously high F_m values and a yield stress given by the elastic limit [e.g., Yogendrakumar et al. (*6*)].

The details of the model parameters are shown in Figure 2. The tangent load modulus D_t on the initial loading curve is calculated as

$$D_t = \frac{dF}{d\varepsilon_a} = \frac{D_i}{[1 + (D_i/F_m)|\varepsilon_a|]^2} \tag{11}$$

The unloading and reloading moduli, D_{ur}, are defined in terms of the initial load modulus as

$$D_{ur} = KD_i \tag{12}$$

where K is a constant.

The unloading and reloading paths are assumed to follow the Masing criterion. The equation for the unloading curve from point $A(\varepsilon_r, F_r)$ or for the reloading curve from point B at which the loading reverses direction is given by

$$\frac{F - F_r}{2} = \frac{D_{ur}(\varepsilon_a - \varepsilon_r)/2}{[1 + (D_{ur}/2F_m)|\varepsilon_a - \varepsilon_r|]} \tag{13}$$

The shape of the unloading-reloading curve is shown in Figure 2. The tangent load modulus at a stress point on an unloading or reloading curve is given by

$$D_t = \frac{dF}{d\varepsilon_a} = \frac{D_{ur}}{[1 + (D_{ur}/2F_m)|\varepsilon_a - \varepsilon_r|]^2} \tag{14}$$

During the analysis, compression is not allowed in the polymeric geosynthetic reinforcement.

To evaluate the accuracy of the proposed nonlinear hyperbolic reinforcement relationship, the model was used to simulate the load-deformation behavior of a typical woven polyester geogrid reinforcement during a rapid cyclic in-isolation tensile test. Figure 3 shows the experimental load-deformation curve together with the predicted response. The three model parameters D_i, F_m, and K used in the simulation were 1000 kN/m, 30 kN/m, and 1.5, respectively. The proposed model appears to simulate satisfactorily not only the initial loading curve but also the subsequent hysteresis loops during cyclic reloading. The rate of loading used in the tensile testing was limited by the capacity of the equipment. The cyclic loading frequency of 0.5 Hz is considered typical for earthquake-induced horizontal motions but is significantly less than that expected during single-pulse air blast loading. However, at the time of writing there was no rapid cyclic loading

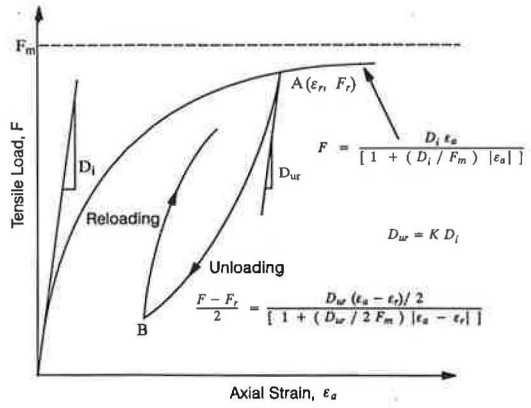

FIGURE 2 Hyperbolic load-strain relationship for polymeric material.

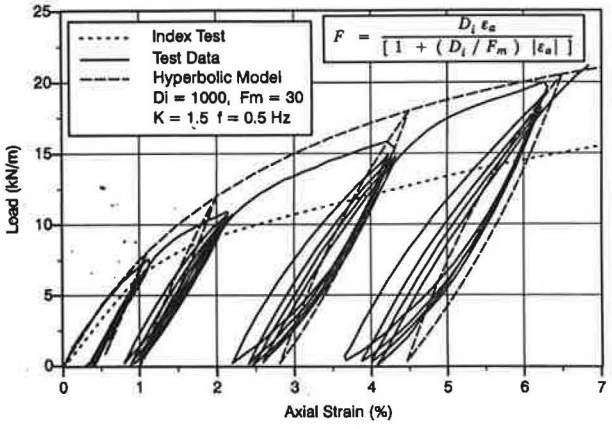

FIGURE 3 Observed and computed load-deformation behavior for woven polyester geogrid.

data available from other sources for this type of geosynthetic. Nevertheless, it is generally known that as the rate of loading of polymeric material increases, the modulus of the material increases and hence the magnitudes of deformations reported in this study are likely conservative (i.e., greater than what may be expected with stiffer modulus values).

Superimposed on Figure 3 is the result of a standard tensile test carried out according to the ASTM 4595 method of test (i.e., 10 percent axial strain/min). As may be expected, the rapid loading test gives a stiffer sample response, suggesting that conventional index test results should not be used directly in simulations modeling rapid excitation of reinforced soil structures.

FINITE ELEMENT ANALYSES

Example Reinforced Soil Wall

Program RESBLAST was used to determine the response of the example reinforced soil wall shown in Figure 4 for a variety of blast loadings. The wall is 6 m high and reinforced with polymeric geogrids 4.8 m long placed horizontally at an equal vertical spacing of 0.75 m. The elevations of the bottom and top reinforcement layers are 0.38 m and 5.63 m, respectively. The geometry of the wall and soil properties have been taken from a retaining wall reported by Richardson (*15*) that was reinforced with steel strips and subjected to seismic excitation from buried explosive charges. The full-scale experimental wall reported by Richardson (*15*) has been modeled using program TARA-3, which is the precursor to program RESBLAST. The predicted dynamic tie forces and accelerations at locations in this wall have been reported by the authors earlier (*9*). The predicted performance was in good agreement with the measured values.

The program RESBLAST models the reinforced soil system as an assemblage of quadrilateral soil elements and one-dimensional beam elements. The finite element representation of the reinforced soil system shown in Figure 4 consisted of 90 soil elements and 32 beam elements. Conventional limit equilibrium methods of design and analysis based on a tie-back wedge method of analysis for internal stability and a gravity structure approach for external stability failure modes indicated that there are adequate factors of safety against instability under static loading conditions (*16,17*).

Blast Pressure–Time Histories

Three RESBLAST analyses were conducted, each representing a different magnitude of blast loading. The blast loading imposed on the reinforced soil wall consisted of a planar blast wave having a magnitude specified by an overpressure ratio and originating 6 m from the front of the wall. The overpressure ratio is defined as the ratio of pressure in excess of ambient pressure (atmospheric pressure) to that of the ambient pressure. Blast waves with a duration of 10 msec and with different overpressure ratios of 3, 5, and 10 were considered in the current analyses, and the computation was continued for 40 msec to ensure return to an equilibrium state. The blast waves are designated as 3 Atm, 5 Atm, and 10 Atm on the figures, and in each case the program SPLIT2D was used to determine the blast pressure–time history at points on the face of the reinforced soil wall. Pressures were converted to forces at each boundary node by multiplying the pressures by the corresponding frontal area, and these forces were used as input to the RESBLAST program.

Figure 5 shows the velocity vector plots obtained from SPLIT2D for the 5 Atm blast wave at times 5.42 and 16.26 msec. At 5.42 milliseconds, the shock front has not struck the retaining wall (Figure 5a). Figure 5b shows the interaction of the wave front with the structure at 16.26 msec.

Figure 6 shows the blast pressure–time histories at two selected boundary nodes (Nodes 2 and 9). It can be seen that in all cases there is an instantaneous increase in pressure followed by a steady decay of pressure. At Node 2, the pressure is amplified by a factor of 3.7, 3.0, and 2.7 for the 10 Atm, 5 Atm, and 3 Atm blast wave, respectively. For each of the cases, amplification of pressures at other boundary locations on the face of the wall fall between the values at Nodes 2 and 9 in rough inverse proportion to height above the toe. As expected from shock propagation theory, the arrival time for the shock front at the wall face diminishes with overpressure ratio.

Model Parameters

Values of K_{2max} and other soil properties used in the RESBLAST analysis for the different soil zones are given in the following table. The load-strain behavior of the polymeric geosynthetic reinforcement under blast conditions is assumed

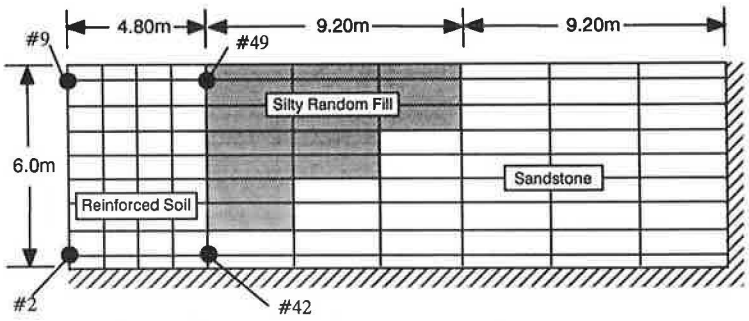

FIGURE 4 Finite element representation of example reinforced soil wall.

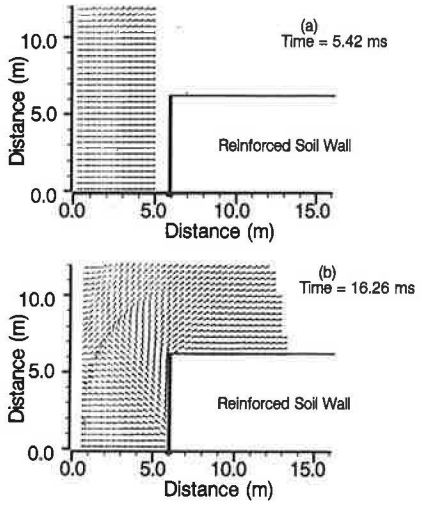

FIGURE 5 Velocity vector plots from SPLIT2D analysis, 5-Atm blast wave.

to be approximated by the hyperbolic form shown in Equation 10. The three model parameters D_i, F_m, and K were taken as 3600 kN/m, 144 kN/m, and 2.0, respectively, and were based on the results of a rapid cyclic in-isolation tensile test carried out at a frequency of 1 Hz on an HDPE uniaxial geogrid.

Type	K_{2max}	*Friction Angle (deg)*	*Unit Weight (kN/m³)*	*Poisson's Ratio*
Select fill	56	38	18.8	0.35
Silty fill	50	36	17.2	0.35
Sandstone	70	38	18.8	0.35

Numerical Results

The horizontal displacement–time histories of Node 2, located close to the base of the wall face, and Node 42, located at the right end of the bottom reinforcement layer, are shown in Figure 7 for different blast loading conditions. The displacement responses of these two nodes are similar in shape and indicate that displacements at these locations generally increase with elapsed time and are largely irrecoverable. As expected, displacements increase with magnitude of the source detonation, and the elapsed time to peak displacement increases with distance from the blast.

Figure 8 shows the horizontal displacement–time histories of Nodes 9 and 49, respectively, for the three different blast loadings. Node 9 is located at roughly the top of the wall face, and Node 49 is located at the free end of the reinforcement layer at the same elevation. Qualitative trends identified for the lower elevation nodes are apparent in these figures, but the magnitude of the horizontal displacements of upper nodes is significantly greater (typically by a factor of 7 to 8).

The axial strain–time histories at two locations, Element 53 close to the face of the wall and Element 56 close to the free end of the near-middle reinforcement layer, are shown in Figure 9. At both locations there was a decrease in the reinforcement tensile strain as the blast loading pulse traveled through the reinforced soil mass. In the case of the 10-Atm blast wave there was evidence of a small increase in tensile strain above the static level during the structure rebound (Figure 9). The maximum peak strain in the reinforcement was about 1 percent during static and blast loading. This strain is well within the yield limit of the material on the basis of the results of rapid cyclic loading of the reinforcement sample in the laboratory and manufacturer's literature on the static load-strain-time properties of the polymeric grid material.

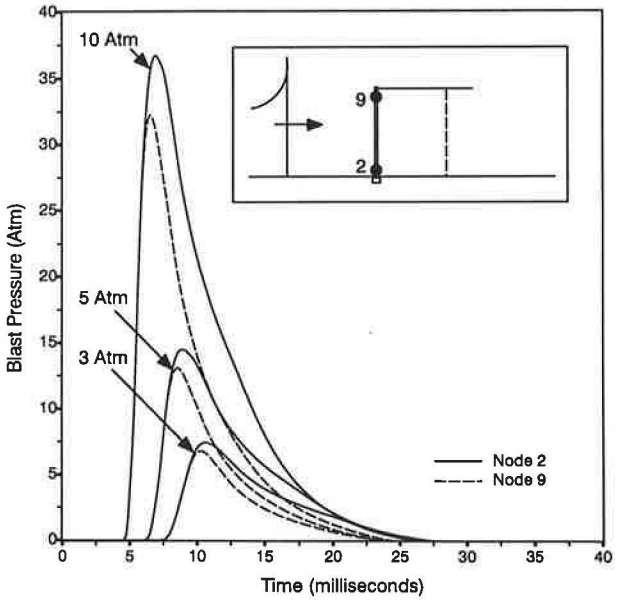

FIGURE 6 Blast pressures at Nodes 2 and 9 from different blast loadings.

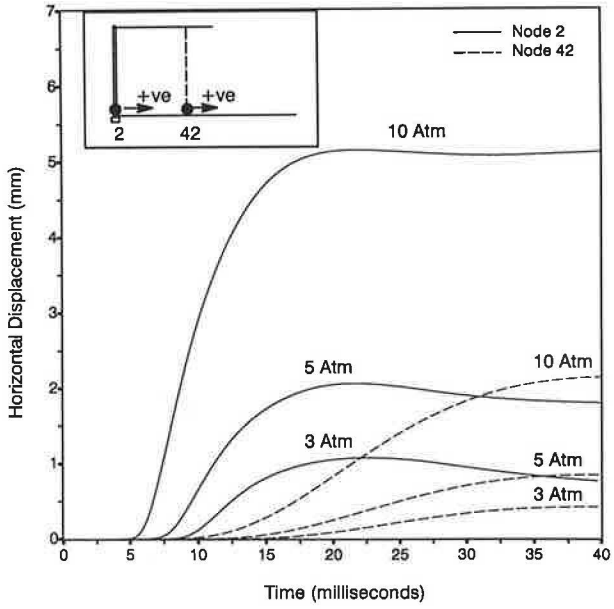

FIGURE 7 Horizontal displacement time histories of Nodes 2 and 42.

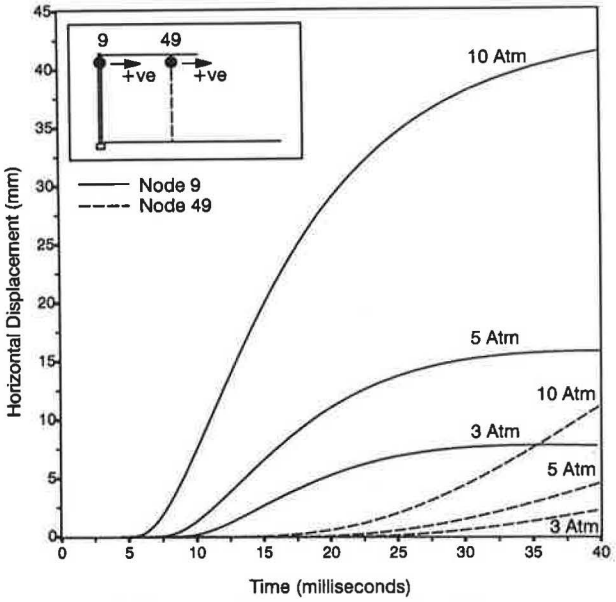

FIGURE 8 Horizontal displacement time histories of Nodes 9 and 49.

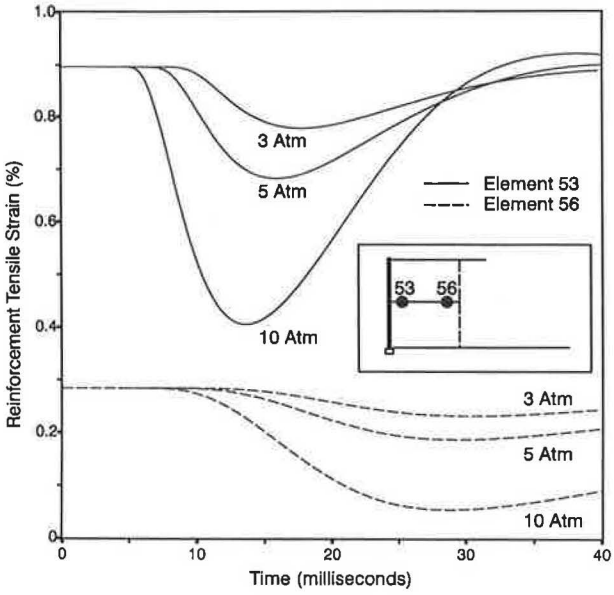

FIGURE 9 Strain time histories of Elements 53 and 56.

Example Steepened Slope

The response of reinforced and unreinforced soil slopes were computed using the RESBLAST program for a given blast loading to examine the influence of the reinforcement. The slopes were assumed to be 6 m high with a side slope of 1:1. The reinforced soil slope was lightly reinforced with 9-m lengths of the same polymeric material used in the previous example. The reinforcement layers were placed horizontally with a vertical spacing of 1 m. The finite element representation of the reinforced soil slope shown in the inset diagram of Figure 10 consisted of 390 soil elements and 90 one-dimensional beam elements. Slip elements, which allow for relative movement between the soil and the reinforcement, were not used in this analysis since the interfacial shear stress between the soil and

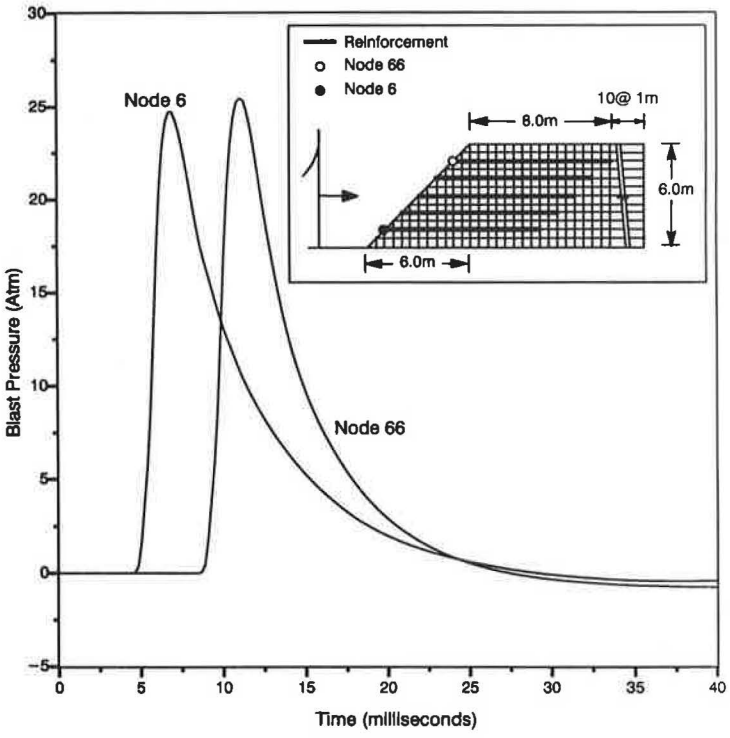

FIGURE 10 Blast pressure time history at Nodes 6 and 66.

the planar reinforcement was assumed to be too small to cause slippage.

Blast pressures caused by a planar blast wave having an overpressure ratio of 10 and a duration of 10 msec and originating at a horizontal distance of 6 m from the toe of the slope were obtained using the SPLIT2D program. Figure 10 shows the blast pressure–time histories at Nodes 6 and 66, which are located on the sloping face at elevations of 1 m and 5 m, respectively. The figure shows that the blast wave causes an average pressure amplification of 2.6 along the sloping side. As expected, the data indicate that the shock front does not arrive at every point on the slope at the same time. The ability to time phase the blast loading at the slope face is one of the distinct advantages of program SPLIT2D.

The following properties were selected for the soil in the slope: K_b = 2950.0, n = 0.5, K_{2max} = 29.0, cohesion = 33 kPa, angle of internal friction = 17 degrees, and unit weight = 20 kN/m^3. These properties were taken from an actual reinforced embankment reported by Scott et al. (*18*). For the polymeric reinforcement, the three model parameters D_i, F_m, and K were taken from the previous example. A static analysis was first conducted to establish the stress-strain field before the blast loading. The program also simulated the incremental construction process of the slope.

Numerical Results

Figure 11 shows the horizontal displacement–time history at Nodes 6 and 66 for the unreinforced and reinforced slopes. Node 66 is located on the face of the structure at an elevation of 5 m close to the crest of the slope. Responses for reinforced and unreinforced cases are similar and show that there are permanent deformations in the structure at the end of loading. The comparison also shows clearly the beneficial effect of the reinforcement in reducing both dynamic and permanent slope deformations.

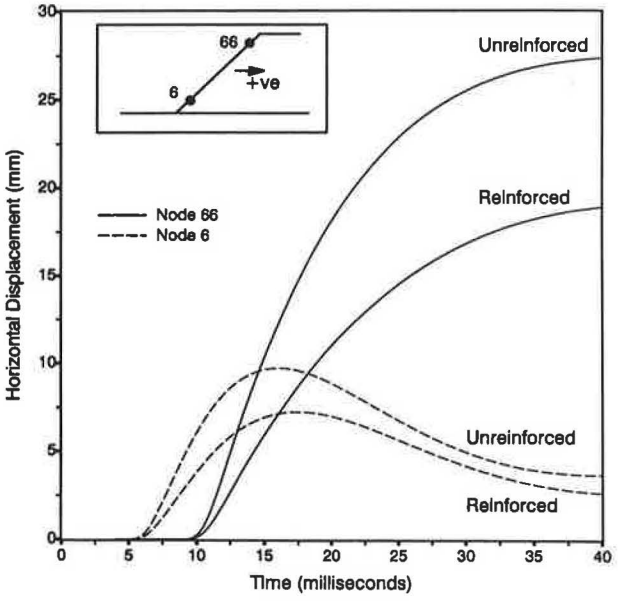

FIGURE 11 Horizontal displacement time histories of Nodes 6 and 66.

The horizontal displacement–time histories of Node 6, located on the face of the slope at an elevation of 1 m are qualitatively different from the response recorded at the top of the slope. Here the displacement at Node 6 reaches a peak value about 12 msec after the shock front has struck. Unlike the higher elevations the soil mass attempts to follow the blast pressure–time excitation. The qualitative differences in response at different locations along the face of the slope example and previous wall example illustrate the important influence of facing geometry on structure response to blast loading.

In summary, the maximum displacement predicted at Nodes 66 and 6 in Figure 11 is reduced to about 70 to 75 percent of the value predicted at the same location in the unreinforced slope.

CONCLUSIONS

The paper has presented the results of a preliminary numerical study of the response of example geosynthetic reinforced soil wall and slope structures to air blast loading. The principal conclusions from this study can be summarized as follows:

1. Program SPLIT2D, which is a code for the prediction of air blast propagation, has proven to be useful for estimating pressure-time response at the boundaries of reinforced soil structures in proximity to aboveground detonation. The program is unique in its ability to predict the variation of pressures on reinforced soil structures and to account for the time phasing of blast loads against inclined surfaces.
2. Program REBLAST may be a useful tool for the simulation of the nonlinear behavior of the soil and polymeric reinforcement in retaining wall and steepened slope structures and for assessing their performance under blast loads in terms of deformations.
3. Rapid cyclic-tensile loading of sample geosynthetic reinforcement showed that the modulus of the geosynthetic depends on both the rate of loading and the magnitude of the accumulated strain. The reinforcement model gave a reasonable estimate of the laboratory load-strain response of the geosynthetic.
4. The lack of structure rebound predicted for the example reinforced soil wall suggests that further straining of the reinforcement beyond the static strain condition may not be a concern.
5. The predicted results for the example slope suggest that the polymeric reinforcement may improve the performance of the structure under blast loading by reducing the magnitude of dynamic and permanent soil deformations by as much as 30 percent. Greater reductions in slope deformation may have been predicted if greater value of reinforcement modulus had been used.

The results of this study are preliminary in nature. Further research is under way to investigate the influence of extensibility of reinforcement material and inclination of the slope face on air blast attenuation. A long-term goal will be the development of computationally simpler limit-equilibrium–

based methods of design and analysis to assess the stability of these structures under single pulse excitation.

ACKNOWLEDGMENTS

The funding for this study was provided by the Department of National Defence (Canada) as part of ongoing research at RMC related to the design and analysis of blast- and seismic-resistant geosynthetic reinforced soil structures. The authors would like to thank Paul Thibault of Combustion Dynamics Limited, Medicine Hat, Alberta, and David Ritzel of Defence Research Establishment, Suffield, Alberta, for their assistance with the SPLIT2D code.

REFERENCES

1. M. A. Yako and B. R. Christopher. Polymerically Reinforced Retaining Walls and Slopes in North America. *Proc., NATO Advanced Research Workshop on Application of Polymeric Reinforcement in Soil Retaining Structures*, Kingston, Ontario, Canada, June 8–12, 1987, pp. 239–283.
2. J. Ferritto, J. Tancreto, and K. Hager. *Design Procedures and Effectiveness of Reinforced Earth Berms for Enhancing Facility Survivability*. Naval Civil Engineering Laboratory, Port Hueneme, Calif., 1988.
3. R. Bonaparte, G. R. Schmertmann, and N. D. Williams. *Seismic Design of Slopes Reinforced with Geogrids and Geotextiles*. Technical Note. The Tensar Corporation, Morrow, Ga., 1986.
4. J. Vrymoed. Dynamic Stability of Soil Reinforced Walls. In *Transportation Research Record 1242*, TRB, National Research Council, Washington, D.C., 1989, pp. 29–38.
5. P. Segrestin and M. J. Bastick. Seismic Design of Reinforced Earth Retaining Walls—The Contribution of Finite Element Analysis. *Proc., International Geotechnical Symposium on Theory and Practice of Earth Reinforcement*, Fukuoka, Japan, Oct. 5–7, 1988, pp. 577–582.
6. M. Yogendrakumar, R. J. Bathurst, and W. D. Liam Finn. Seismic Response of Reinforced Soil Retaining Walls. *Proc., Seventh Conference of the International Association for Computer Methods and Advances in Geomechanics*, Cairns, Australia, May 6–10, 1991, pp. 907–912.
7. M. Yogendrakumar, R. J. Bathurst, and W. D. Liam Finn. Response of Reinforced Soil Walls to Earthquake Loads. *Proc., 9th Panamerican Conference*, Vina del Mar, Chile, Aug. 1991.
8. M. Yogendrakumar, R. J. Bathurst, and W. D. Liam Finn. Response of Reinforced Soil Slopes to Earthquake Loadings. *Proc., Sixth Canadian Conference on Earthquake Engineering*, Toronto, Ontario, Canada, June 12–14, 1991, pp. 445–452.
9. M. Yogendrakumar, R. J. Bathurst, and W. D. Liam Finn. Dynamic Response Analysis of a Reinforced Soil Retaining Wall. *Geotechnical Journal*, ASCE (in press).
10. *SPLIT2D—Version 4.3:A 2-D Hydrocode for Blast Loading on Arbitrary Shapes*, Combustion Dynamics Ltd., Medicine Hat, Alberta, Canada, 1990.
11. M. Yogendrakumar and R. J. Bathurst. *RESBLAST: A Computer Program to Compute the Response of 2-D Reinforced Soil Systems to Blast Loadings*. Department of Civil Engineering, Royal Military College of Canada, Kingston, Ontario, Canada, 1990.
12. W. D. Liam Finn, M. Yogendrakumar, N. Yoshida, and H. Yoshida. *TARA-3: A Program to Compute the Response of 2-D Embankments and Soil-Structure Interaction Systems to Seismic Loading*. Department of Civil Engineering, University of British Columbia, Vancouver, Canada, 1986.
13. H. B. Seed and I. M. Idriss. *Soil Moduli and Damping Factor for Dynamic Response Analysis*. Report EERC 70-10. Earthquake Engineering Research Center, University of California, Berkeley, 1970.
14. R. B. Goodman, R. E. Taylor, and T. L. Brekke. A Model for the Mechanics of Jointed Rock. *Journal of the Soil Mechanics and Foundations Division*, ASCE, Vol. 94, No. SM3, 1968, pp. 637–659.
15. G. N. Richardson. *The Seismic Design of Reinforced Earth Walls*. School of Engineering and Applied Science, University of California, Los Angeles, 1976.
16. B. R. Christopher and R. D. Holtz. *Geotextile Design and Construction Guidelines*. National Highway Institute, Washington, D.C., 1989.
17. R. J. Bathurst. Geosynthetics for Reinforcement Applications in Retaining Walls. *Proc., 44th Canadian Geotechnical Conference*, Vol. 2, Paper 74, Calgary, Alberta, Canada, Sept. 29–Oct. 2, 1991.
18. J. D. Scott, D. C. Sego, E. A. Richards, B. A. Hoffman, and E. R. Burch. Design of the Devon Geogrid Test Fill. *Geosynthetics Conference '87*, Vol. 1, New Orleans, La., 1987, pp. 157–168.

Publication of this paper sponsored by Committee on Transportation Earthworks.